

## Synthesis of Yb-doped $\text{Sc}_2\text{O}_3$ nanocrystalline powders

**A.C. Bravo\***, **L. Longuet\***, **D. Autissier\*** et **J.F. Baumard\*\***

(\***Commissariat à l’Energie Atomique, BP 16, 37260 Monts, France**

(\*\***Laboratoire Science des Procédés Céramiques et de Traitements de Surface, SPCTS, UMR CNRS 6638, 47-73 avenue Albert Thomas, 87065 Limoges Cedex, France**

### Abstract

We report the preparation of nanocrystalline  $\text{Yb}:\text{Sc}_2\text{O}_3$  powders with an ultimate intent to make transparent  $\text{Yb}:\text{Sc}_2\text{O}_3$  ceramics for laser applications. Precursors were synthesized by a coprecipitation method from a mixed solution of scandium and ytterbium nitrates using aqueous ammonium hydrogen carbonate as precipitant. The effects of the precipitation process on the powders’ characteristics were studied. The phase evolution, the structure and the morphological characteristics of the different precipitates and calcined precursors were studied by means of TG/DTA, XRD and SEM methods. Carbonate precursors were transformed into pure  $\text{Yb}:\text{Sc}_2\text{O}_3$  phase after a thermal treatment  $\geq 700^\circ\text{C}$  for 2 hours. The particles of the as-prepared nanocrystalline  $\text{Yb}:\text{Sc}_2\text{O}_3$  powders are spherical and narrow size distributed. Their average diameter is lower than 50nm.

**Keywords:** Chemical synthesis, Transparent ceramic,  $\text{Yb}:\text{Sc}_2\text{O}_3$ .

### Introduction

Transparent polycrystalline ceramics, with optical and mechanical properties similar to their single crystals, turn out to be a very interesting alternative for laser materials. Indeed, they present several advantages such as easiness in fabrication of pieces of desired shape and size, flexible concentration doping and low-cost for mass production. Rare earth sesquioxides are encouraging hosts for solid-state lasers [1]. Scandium sesquioxide doped with  $\text{Yb}^{3+}$  presents very interesting laser properties [2].

To fabricate high-performance  $\text{Yb}:\text{Sc}_2\text{O}_3$  transparent ceramics, the synthesis of high-quality  $\text{Yb}:\text{Sc}_2\text{O}_3$  powders is a key point of the process. The starting powders must present specific characteristics. The size, the morphology and the agglomeration state of the particles influence in an important way the density and the microstructure of the sintered material. The powder purity determines the transparency degree after sintering. A chemical powder synthesis allows to elaborate powders with a very great purity. Several chemical routes including precipitation method [3-6], combustion synthesis [7-8], sol-gel processing [9], hydrothermal method [10], emulsion synthesis... have been developed and already been employed for the fabrication of rare earth doped garnets and sesquioxides

nanocrystalline powders. They allow to overcome the pollution generally encountered in traditional solid-state reaction process. Among these techniques, the coprecipitation using inorganic salts has been devised as a relatively easy, reliable and inexpensive route to prepare reactive, pure and homogeneous powders.

In this paper, we report the preparation of  $\text{Yb}:\text{Sc}_2\text{O}_3$  precursors by a coprecipitation route. Scandium and ytterbium nitrates were used as the starting materials and aqueous ammonium hydrogen carbonate as the precipitant. The effects of different parameters of the precipitation process (the precipitation technique, the molar ratio between the reactants and the synthesis temperature) and the influence of the calcination temperature on the morphology, the size and the agglomeration state of the scandia powders were investigated.

### Experimental

#### *Synthesis of the $\text{Yb}:\text{Sc}_2\text{O}_3$ precursors*

$\text{Yb}:\text{Sc}_2\text{O}_3$  precursors were prepared by coprecipitation using  $\text{Sc}(\text{NO}_3)_3 \cdot 5\text{H}_2\text{O}$  (99.99%, Metall Rare Earth Limited),  $\text{Yb}(\text{NO}_3)_3 \cdot 5\text{H}_2\text{O}$  (99.9%, Strem Chemicals) and ammonium hydrogen carbonate further noted “AHC” ( $\text{NH}_4\text{HCO}_3$ , 99.9%, Rectapur VWR Prolabo) as starting materials. The salt solution was obtained by dissolving simultaneously  $\text{Sc}(\text{NO}_3)_3 \cdot 5\text{H}_2\text{O}$  and  $\text{Yb}(\text{NO}_3)_3 \cdot 5\text{H}_2\text{O}$  in deionized water to have a concentration of  $\text{Sc}^{3+}$  and  $\text{Yb}^{3+}$  of 0.1M and 0.001M respectively. The aqueous solution of 1.0M  $\text{NH}_4\text{HCO}_3$  was also prepared by dissolution in deionized water. Either the precipitating agent was introduced into the mixed nitrate solution (direct striking method) or the salt solution was added to the precipitant (reverse striking method) under magnetic stirring with a dropping rate of 3mL/min. After completing the reaction, the precipitate slurry was aged for 3 hours with continuous stirring. The precipitate was then separated by centrifugation and washed several times with deionized water to completely remove  $\text{NH}_4^+$ ,  $\text{NO}_3^-$  and  $\text{OH}^-$  by-products. After washing, the cake was dried at  $60^\circ\text{C}$  for one night and then calcined in air at various temperatures in the range  $400^\circ\text{C}$ - $1100^\circ\text{C}$  for 2 hours with a heating rate of  $150^\circ\text{C}/\text{h}$  to form the oxide phase. Some previous works, focused on the precipitation synthesis of garnets [11-12] and sesquioxides nanocrystalline powders [13-17], reported that the

precursors' characteristics could vary with different parameters of the precipitation process. We have chosen to study the effects of three of them. Indeed (i) the precipitation technique, (ii) the molar ratio R with  $R = \text{AHC}/\text{Sc}^{3+}$  and (iii) the synthesis temperature seem to have an important effect on the nature, the size, the morphology and the agglomeration state of the precipitates' particles. In this work, two precipitation techniques (direct and reverse striking precipitations), three molar ratio ( $R=3, 4$  or  $5$ ) and two synthesis temperatures (room temperature or  $40^\circ\text{C}$ ) were employed.

### Characterizations

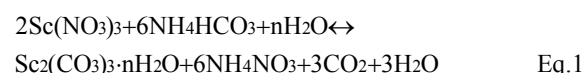
The approximate composition of the precipitates and the purity degree of the powders were determined by chemical analysis (ICP-AES: Horiba Jobin Yvon Model Activa, ICP-MS: Thermoelectron Serie X7). Phase identification was performed by the X-ray powder diffraction method (XRD) on a D5000 X-ray diffractometer using  $\text{CoK}_{\alpha 1,2}$  radiation. The average crystallite size of the  $\text{Yb}:\text{Sc}_2\text{O}_3$  powders at the different calcination temperatures was determined from the XRD line broadening (the full width half maxima, FWHM) of the more intense peaks using Scherrer equation. The morphology, the size and the agglomeration state of the precipitates and the calcined powders particles were observed by scanning electron microscopy with field emission gun (SEM-FEG) (Zeiss DSM 982 Gemini). The Brunauer-Emmett-Teller (BET) surface areas of the powders were measured on a specific surface area analyser (Micromeritics ASAP 2010). Thermal behaviours of the precursors were studied with TG-DTA thermal analyser (Setaram TAG 24) with a heating rate of  $10^\circ\text{C}/\text{min}$  in air. All the experiments were realized at room temperature.

## Results and Discussion

### Precipitation of the $\text{Yb}:\text{Sc}_2\text{O}_3$ precursors

The approximate composition of the different precipitates was determined from the chemical analysis results. These are carbonates (Table 1 and Table 2) of composition  $\text{Yb}_{0,01}\text{Sc}(\text{CO}_3)_x(\text{NH}_4)_y(\text{OH})_z \cdot n\text{H}_2\text{O}$  with  $x, y, z$  and  $n$  depending on the synthesis conditions employed. The precursors were of high purity. It was noticed that the several washings were not always enough to completely remove the  $\text{NH}_4^+$  by-products.

The composition of the precipitates is determined by the competition between the hydroxyls and carbonate anions. During the precipitation, the two following chemical reactions can occur: [13]



Molar ratio	Synthesis temperature	Approximate composition (with $\text{Yb}_{0,01}$ )
R3	Room temperature	$\text{Sc}(\text{OH})_{1,52}(\text{CO}_3)_{0,76} \cdot 1,53\text{H}_2\text{O}$
R4		$\text{Sc}(\text{CO}_3)_{3,06}(\text{NH}_4)_{1,40} \cdot 2,38\text{H}_2\text{O}$
R5		$\text{Sc}(\text{OH})_{2,09}(\text{CO}_3)_{0,48} \cdot 0,22\text{H}_2\text{O}$
R3	$40^\circ\text{C}$	$\text{Sc}(\text{OH})_{1,86}(\text{CO}_3)_{0,58} \cdot 0,92\text{H}_2\text{O}$
R4		$\text{Sc}(\text{OH})_{0,61}(\text{CO}_3)_{1,49}(\text{NH}_4)_{0,56} \cdot 1,33\text{H}_2\text{O}$
R5		$\text{Sc}(\text{OH})_{0,16}(\text{CO}_3)_{1,87}(\text{NH}_4)_{0,86} \cdot 1,25\text{H}_2\text{O}$

Table 1: approximate composition of direct striking precipitates

Molar ratio	Synthesis temperature	Approximate composition (with $\text{Yb}_{0,01}$ )
R3	Room temperature	$\text{Sc}(\text{OH})_{0,37}(\text{CO}_3)_{1,73}(\text{NH}_4)_{0,79} \cdot 1,36\text{H}_2\text{O}$
R4		$\text{Sc}(\text{CO}_3)_{2,10}(\text{NH}_4)_{1,53} \cdot 1,53\text{H}_2\text{O}$
R5		$\text{Sc}(\text{OH})_{2,27}(\text{CO}_3)_{0,38}$
R3	$40^\circ\text{C}$	$\text{Sc}(\text{OH})_{1,50}(\text{CO}_3)_{0,78} \cdot 0,44\text{H}_2\text{O}$
R4		$\text{Sc}(\text{CO}_3)_{1,99}(\text{NH}_4)_{0,99} \cdot 1,25\text{H}_2\text{O}$
R5		$\text{Sc}(\text{OH})_{1,95}(\text{CO}_3)_{0,53} \cdot 0,61\text{H}_2\text{O}$

Table 2: approximate composition of reverse striking precipitates

Thus, with the presence of  $\text{OH}^-$  and  $\text{CO}_3^{2-}$  anions in the system,  $\text{Sc}_2(\text{CO}_3)_3$  and  $\text{Sc}(\text{OH})\text{CO}_3$  can precipitate according to Eq.1 and Eq.2.

The XRD results show that the direct striking precipitates with a R3 molar ratio are amorphous carbonates whereas those prepared otherwise are crystallized carbonates. The two types of X-ray diffraction patterns observed are presented in Fig.1. No JCPDS Card corresponds to the XRD pattern in Fig.1(b). Nevertheless, it is similar to those presented by Li et al. [15] for carbonates of similar compositions.

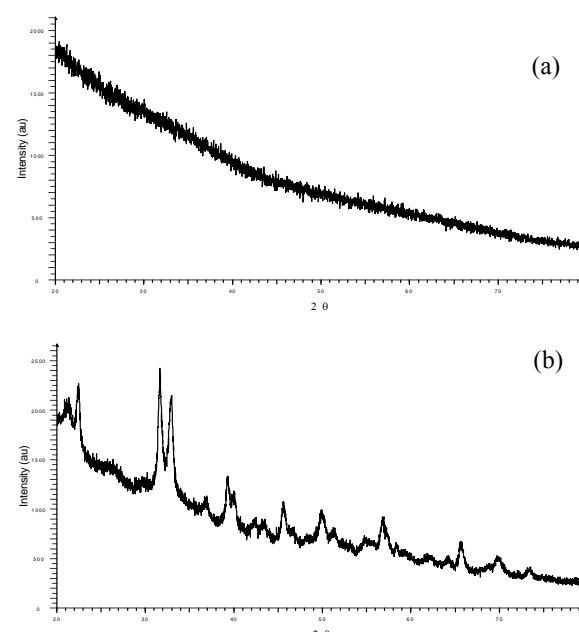


Fig.1: XRD patterns of  $\text{Yb}:\text{Sc}_2\text{O}_3$  precursor powders (a) amorphous precipitates, (b) crystallized precipitates

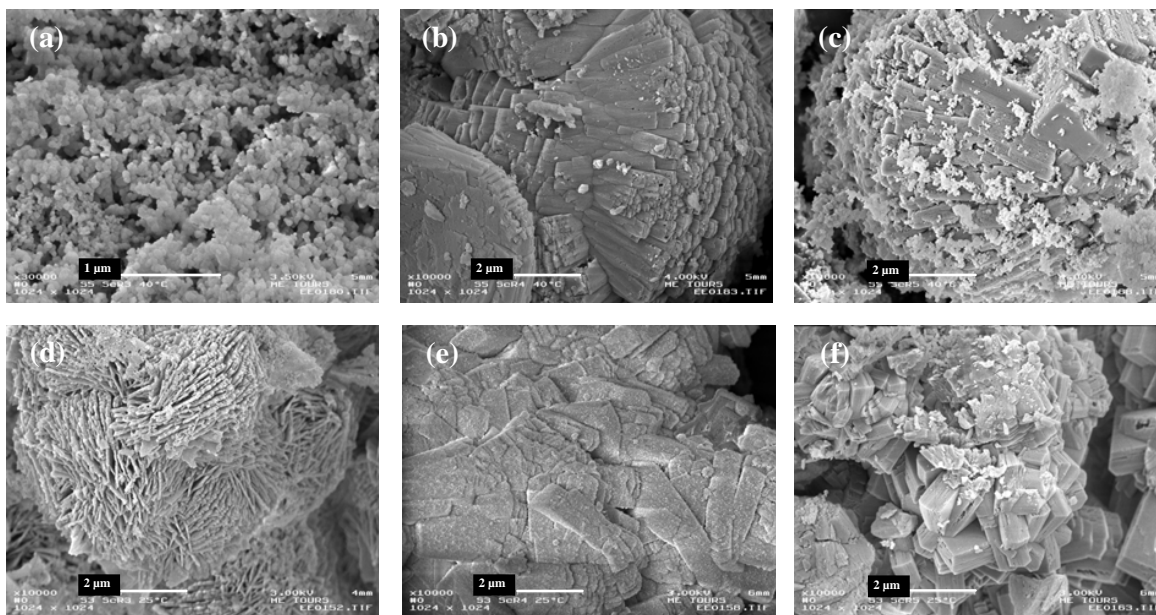


Fig.2: field emission scanning electron micrographs of precursor powders synthesized at 40°C direct striking method from (a) to (c) and reverse striking method from (d) to (f) molar ratio R3 for (a) and (d), R4 for (b) and (e), R5 for (c) and (f)

The morphological characteristics of the precipitates are influenced by the precipitation conditions such as the molar ratio and the striking methods. SEM micrographs indicate that the amorphous carbonates, which are the R3 precipitates synthesized by direct striking method at room temperature and 40°C, are composed of spherical nanoparticles that are relatively large-sized distributed and agglomerated (Fig.2(a)). On the contrary, the crystallized carbonates are flakes-like and become more equiaxed when the molar ratio increases (Fig.2(b-f)). It was noticed that the final pH value of the slurry was higher than 6 for all the preparations except for the R3 direct striking synthesis where the pH value was lower. We can suppose that the crystallinity and the morphological characteristics of the precipitates depend on the final pH value and that the formation of crystallized precipitates composed of flakes-like particles is supported by a pH value higher than 6.

#### Thermal behaviour of the precursors

The mechanisms of thermal decomposition of the different precursors were studied by TG/DTA analyses. The thermal decomposition of crystallized carbonates consists in two distinct steps (Fig.3(a)). First, an endothermal peak associated to a fast and important weight loss (almost the overall weight loss) around 200°C is due to the removal of absorbed water, crystalline H<sub>2</sub>O and NH<sub>3</sub>. Then, an exothermal peak around 475°C can be attributed to the crystallization into Sc<sub>2</sub>O<sub>3</sub> phase. In this case, the overall weight loss is around 65%.

The thermal decomposition of an amorphous carbonate is quite different (Fig.3(b)). Large endothermal peaks around 150°C and 550°C are associated to a more progressive weight loss. The TG/DTA curves show a complete decomposition of the precursor into scandium oxide at a higher temperature. Indeed, the peak

attributed to the crystallization into Sc<sub>2</sub>O<sub>3</sub> appears around 570°C. In the case of an amorphous carbonate, the exothermal phenomenon is associated to a weight loss and the overall weight loss is lower than that for a crystallized carbonate.

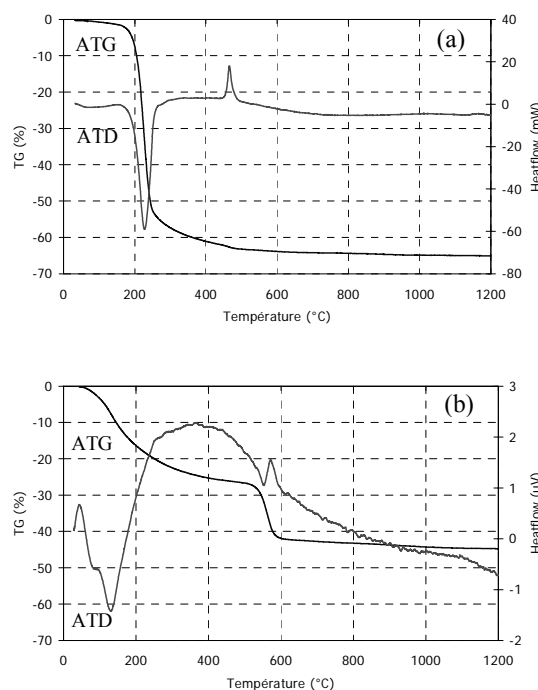


Fig.3: TG and DTA curves (a) crystallized precipitate, (b) amorphous precipitate

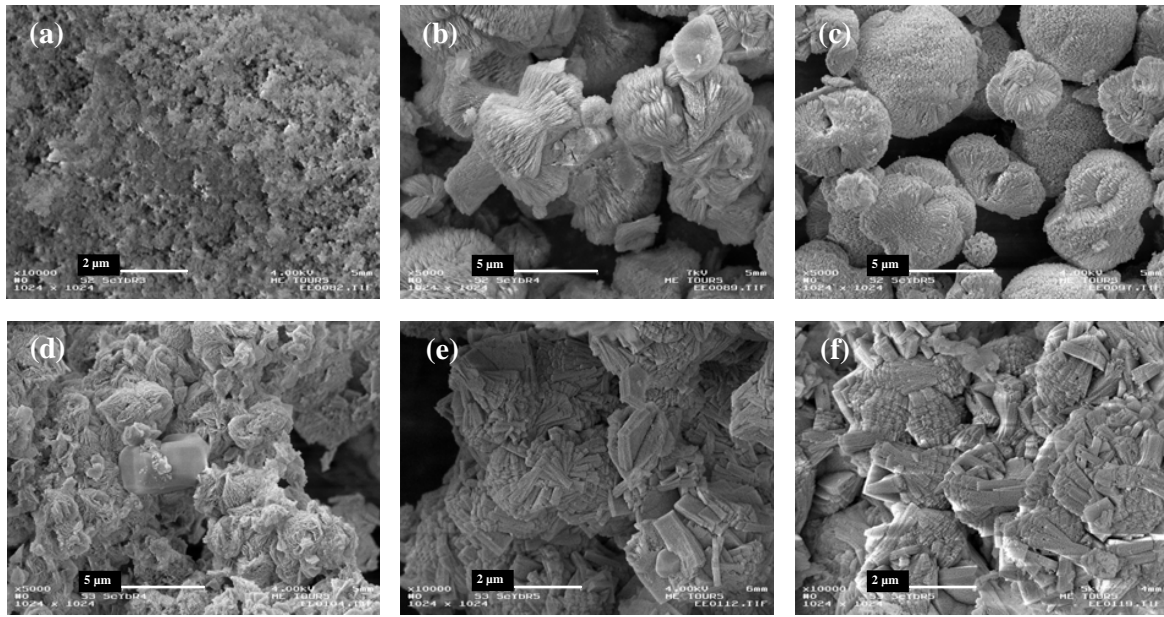


Fig.4: field emission scanning electron micrographs of precursor powders synthesized at 25°C and calcined at 700°C for 2h - direct striking method from (a) to (c) and reverse striking method from (d) to (f) molar ratio R3 for (a) and (d), R4 for (b) and (e), R5 for (c) and (f)

#### Calcination of the precursors

According to the previous results, the two types of precursors transform into  $\text{Sc}_2\text{O}_3$  phase above 600°C. Consequently, they were calcined for 2 hours at various temperatures in the range 700°C-1100°C to produce doped scandia powders. The effects of the three studied parameters on the morphological characteristics were observed.

A synthesis temperature of 40°C seems to have no influence on the morphology, the size or the agglomeration state of the powders' particles. Consequently are only presented on Fig.4 and Fig.5 the field emission scanning electron micrographs of powders synthesized at 25°C.

Except in the case of the R3 direct striking synthesis, the crystallites are fairly discrete and spherical in shape (Fig.5). Their average diameter is lower than 50nm after a heat treatment at 700°C. Depending on the calcined powders, the BET surface area vary from 28m<sup>2</sup>/g to 37m<sup>2</sup>/g. If we suppose that the particles are spherical in shape and homogeneous in size, we can determine the equivalent BET diameter  $d_{\text{BET}}$  from the BET surface area  $S_{\text{BET}}$ . The relationship between  $S_{\text{BET}}$  and  $d_{\text{BET}}$  is as follows:

$$d_{\text{BET}} = \frac{6 \cdot 10^3}{S_{\text{BET}} \cdot \rho} \quad \text{Eq.3}$$

With a theoretical density  $\rho$  of 3.86g/cm<sup>3</sup> for  $\text{Sc}_2\text{O}_3$  and a BET surface area of 30m<sup>2</sup>/g, the equivalent BET diameter  $d_{\text{BET}}$  is around 50nm. This result is in agreement with the size of the particles observed on the field emission scanning electron micrographs of Fig.5.

The crystallites form almost spherical objects of 5μm in size when the direct striking method is employed (Fig.4 (b-c)) and platelets of 1 to 2μm in size in case of reverse striking synthesis (Fig.4 (d-f)).

Calcined powders contain no greater impurities. Only traces of sodium were detected in some of them by EDS analysis and explain the presence of a sodium chloride crystal in the powder sample (d) of Fig.4. A progressive abrasion of the glass beaker containing the slurry during the synthesis was observed. It is due to the friction induced by the magnetic stirrer. The presence of sodium chloride in some preparations was related to this abrasion.

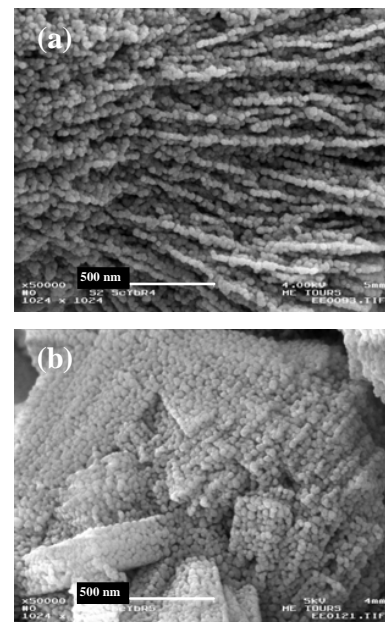


Fig.5: field emission scanning electron micrographs of precursor powders synthesized at 25°C and calcined at 700°C for 2h (a) molar ratio R4 and direct striking method (b) molar ratio R5 and reverse striking method

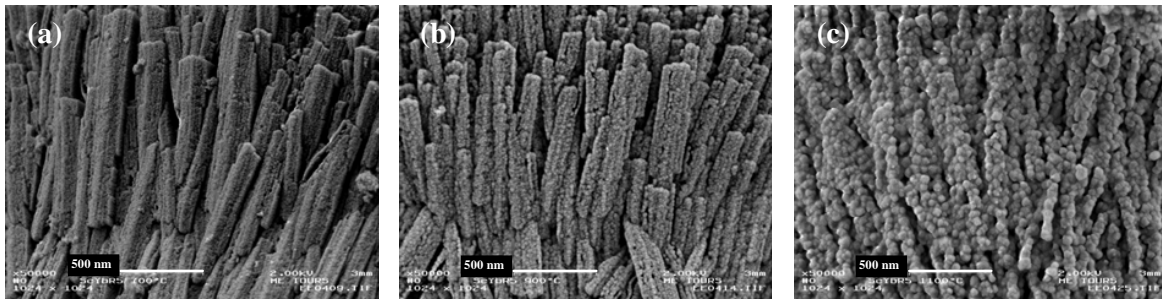


Fig.7: field emission scanning electron micrographs of Yb:Sc<sub>2</sub>O<sub>3</sub> nanocrystalline powders obtained after calcination of the R5 precipitate synthesized at 40°C with the normal striking method (a) 700°C, (b) 900°C, (c) 1100°C

#### *Influence of the calcination temperature on the scandia powders' characteristics*

The following results concern the elaboration of nanocrystalline Yb:Sc<sub>2</sub>O<sub>3</sub> powders from crystallized carbonate precursors such as the R4 and R5 precipitates synthesized at 40°C with the direct or the reverse striking method. The R3 precipitates were not studied longer because of the important agglomeration of its particles after thermal treatment. A mechanical stirring was preferred to a magnetic one which induced abrasion of the beaker and consequently pollutions, as it has been presented above.

R4 and R5 precipitates synthesized at 40°C with the two precipitation techniques were calcined at various temperatures in the range 400°C-1100°C, in order to observe the effects of the heat treatment on the morphological characteristics of the final powders and consequently on their sinterability.

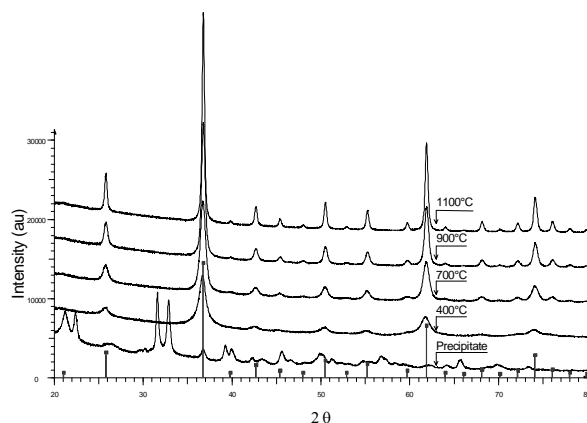


Fig.6: XRD patterns of the R5 precipitate synthesized at 40°C with the normal striking method and calcined at various temperatures

Fig.6 shows the XRD patterns of the R5 precipitate synthesized at 40°C with the normal striking method and the calcined powders at 400°C, 700°C, 900°C and 1100°C respectively. Cubic Sc<sub>2</sub>O<sub>3</sub> crystalline phase is obtained around 400°C and no other crystalline phase is detected. The XRD peaks of the powders calcined above 400°C are indexed with the Sc<sub>2</sub>O<sub>3</sub> JCPDS Card

N°00-042-1463. The crystallization temperature is lower than the one reported by the DTA analysis which indicates a crystalline temperature of Sc<sub>2</sub>O<sub>3</sub> phase at about 475°C. This difference can be explained by a phenomenon of temperature hysteresis. The peaks become higher and sharper when the calcination temperature increases, implying a particle growth of the Yb-doped scandia powders. The average crystallite size can be estimated from the powder diffraction data using Scherrer equation. It increases from 15nm to about 40nm when the calcination temperature increases from 700°C to 1100°C.

Fig.7 shows SEM micrographs of the Yb:Sc<sub>2</sub>O<sub>3</sub> nanocrystalline powders obtained after heat treatment of the same precursor at 700°C, 900°C and 1100°C. The crystallites are discrete, fairly uniform and spherical in shape. They always form micronic platelets like those presented in the previous micrographs. Their size increases with the calcination temperature from 15-20nm at 700°C to 40-60nm at 1100°C.

The BET surface areas of the various calcined powders were measured to estimate the equivalent BET diameter of their particles. As it could be expected, the BET surface area decreases when the calcination temperature increases. Consequently, the equivalent BET diameter increases. The whole data concerning the particle size analysis are summarized in Table 3.

Sintering temperature	700°C	900°C	1100°C
BET surface area (m <sup>2</sup> /g)	86	42	24
Equivalent BET diameter (nm)	18	35	64
Average XRD crystalline size (nm)	15	25	35-40
SEM particle size (nm)	15-20	25-30	40-60

Table 3: Yb:Sc<sub>2</sub>O<sub>3</sub> nanocrystalline powders obtained after calcination of the R5 precipitate synthesized at 40°C with the normal striking method

The differences between the particle sizes calculated from the XRD patterns and the BET surface area data and those observed on the SEM micrographs can be explained by the measure incertitude and the resolution of instrumentation.

## Conclusion

Nanocrystalline Yb:Sc<sub>2</sub>O<sub>3</sub> powders were prepared by a coprecipitation method from a mixed solution of scandium and ytterbium nitrates and using ammonium hydrogen carbonate as precipitant. The precipitation process was optimized in order to prepare reactive, pure and homogeneous Yb-doped scandia powders with an ultimate intent to make transparent ceramics for laser application. The effects of the precipitation process on the powders' characteristics were studied.

It was observed that the precipitation conditions such as the striking methods, the temperature synthesis and particularly the molar ratio, influence the composition and the morphology of the precursors. The R3 direct striking precipitates are amorphous and the scandia powders obtained after calcination are agglomerated. In consequence, they don't suit with our application. On the contrary, precipitates elaborated with a higher molar ratio (R4 or R5) are crystallized and allow to produce nanocrystalline, narrow-size distributed and loosely agglomerated scandia powders after a thermal treatment  $\geq 700^\circ\text{C}$ . Their average diameter is lower than 50nm.

## Acknowledgements

The authors thank the researchers for their contribution to the chemical and microstructural characterizations of the materials.

## References

- [1] K. Petermann, *J. Lumin.*, 87-89 (2000), 973-975
- [2] J. Lu, *Appl. Phys. Lett.*, 83, 6 (2003), 1101-1103
- [3] D.J. Sordelet, *J. Am. Ceram. Soc.*, 71, 12 (1988) 1148
- [4] T. Ikegami, *J. Ceram. Soc. Jpn, Int. Ed.* 107 (3) (1999) 297
- [5] N. Saito, *J. Am. Ceram. Soc.* 81, 8 (1998) 2023
- [6] C.J.J. Tool, *Solid State Ionics* 32/33 (1989) 691
- [7] W.J. Kim, *J. Mater. Sci. Lett.* 18 (1999) 411
- [8] S. Toy, *J. Mater. Res.* 14 (4) (1999) 1524
- [9] R. Subramanian, *Mater. Lett.* 48 (2001) 342
- [10] P.K. Sharma, *J. Mater. Sci. Lett.* 17 (1998) 823
- [11] X. Li, *Opt. Mater.*, 29, (2007) 528
- [12] Ch. Su, *J. Rare Earth*, 23, (2005) 716
- [13] L. Wen, *Opt. Mater.*, 29, (2006) 239
- [14] J. Mouzon, *J. Euro. Ceram. Soc.*, 27, (2007) 1991
- [15] J.G. Li, *J. Am. Ceram. Soc.*, 88 [4], (2005) 817
- [16] J.G. Li, *J. Mater. Res.*, 18 [8], (2003) 1816
- [17] J.G. Li, *J. Am. Ceram. Soc.*, 86 [9] (2003) 1493